Modification of the Electrostatic Environment Is Tolerated in the Oxyanion Hole of the Cysteine Protease Papain†

Robert Ménard,* Céline Plouffe, Pierre Laflamme, Thierry Vernet, Daniel C. Tessier, David Y. Thomas, and Andrew C. Storer

Biotechnology Research Institute, National Research Council of Canada, 6100 Avenue Royalmount, Montréal, Québec, H4P 2R2, Canada

Received September 19, 1994®

ABSTRACT: The oxyanion hole in cysteine and serine proteases can be viewed as an arrangement of prealigned dipoles that complements the changes in charge distribution during the enzymatic reaction. Because of the electrostatic nature of the interaction involved in the oxyanion hole, the introduction of charged residues in that region could have a major effect on the catalytic properties of the enzyme. In this study, residue Gln19, which contributes to one of the hydrogen bonds in the oxyanion hole of papain, has been replaced by glutamic acid, histidine, and asparagine residues. These mutations result in 65−315-fold decreases in k_{cat}/K_M, supporting our previous finding that the side chain of Gln19 contributes to transition state stabilization in the oxyanion hole of papain (Ménard et al., 1991a). Since papain is active over a wide range of pH values, the influence of side chain ionization on activity could be measured quantitatively with the mutant Gln19Glu. The pH dependency of k_{cat}/K_M for Gln19Glu is not of the classical bell-shaped form normally observed for papain, but instead is modulated by ionization of the Glu19 side chain with a pK_a of 6.02. The Gln19Glu mutant at low pH, where the Glu19 side chain is neutral, is the enzyme that displays activity closest to that of wild-type enzyme, with a $(k_{cat}/K_M)_1^{lim}$ value only 20-fold lower than that for papain. As expected, the activity of the Gln19Glu mutant decreases when the Glu19 side chain ionizes. However, introduction of the negatively charged glutamate into the oxyanion hole of papain leads to a further reduction in activity of only 12-fold, and this mutant is still more active than the Gln19Ser enzyme and only 3-fold less active than Gln19Asn. Mutation of Gln19 to His caused the strongest decrease in k_{cat}/K_M of the three mutants, a possible consequence of conformational and ion pair stability perturbations. Contrary to the Gln19Glu enzyme, ionization of His19 could not be detected unambiguously. Probable side chain orientations in the mutants were obtained from molecular modeling experiments, and factors affecting the electrostatic environment of the active site of papain are discussed. Comparison of our results with those obtained for a number of subtilisin mutants indicates that transition state stabilization through oxyanion hole interactions might be more important in serine proteases than in cysteine proteases by approximately 0.5−1.0 kcal/mol.

The hydrolysis of substrates by serine and cysteine proteases is considered to proceed via the formation of tetrahedral intermediates or transition states accompanied by the development of negative charge on the carbonyl oxygen of the substrate. The efficiency of the enzyme in promoting catalysis is related to its ability to stabilize this inherently unstable intermediate. For both serine and cysteine proteases, part of the stabilization is provided by a region of the enzyme that has been termed the oxyanion hole (Henderson, 1970; Robertus et al., 1972; Drenth et al., 1975). An impressive amount of experimental data is available to support the involvement of the oxyanion hole in the catalytic mechanism of serine protease [see Ménard and Storer (1992) for a review]. Numerous crystal structures of serine protease complexes with inhibitors or other compounds that mimic the tetrahedral intermediate are available. These structures provide information from which the two hydrogen bond donors that can interact with the oxyanion of the intermediate can be identified (Ménard & Storer, 1992). One hydrogen bond is contributed by the amide group of the catalytic serine residue, while the second one is provided by the backbone amide of a glycine in trypsin-like proteases or the side chain of an asparagine in subtilisin-like proteases (Henderson, 1970; Robertus et al., 1972). Site-directed mutagenesis experiments performed on subtilisin have allowed the quantitative evaluation of the contribution of this asparagine residue (Asn155) to the catalytic mechanism of the enzyme (Bryan et al., 1986; Wells et al., 1986; Carter & Wells, 1990). Mutation of residue 155 leads to destabilization of the transition state relative to the ground state by 2−5 kcal/mol, and the lack of a significant effect on the dissociation constant of the Michaelis complex (K_s) indicates that the oxyanion hole plays a role mainly in catalysis and not in binding of the substrate.

A similar arrangement of hydrogen bond donors forming an oxyanion hole was found to be present in the X-ray structure of a complex between the cysteine protease papain and a peptide chloromethane inhibitor (Drenth et al., 1975, 1976). As with the serine proteases, the amide group of the catalytic residue (Cys25) contributes to one of the two

† NRCC Publication Number 38474.

* Author to whom correspondence should be addressed.

® Abstract published in *Advance ACS Abstracts,* December 15, 1994.

0006-2960/95/0434-464$09.00/0 Published 1995 by the American Chemical Society

hydrogen bonds in the oxyanion hole of cysteine proteases. The second hydrogen bond donor is located on the side chain of Gln19. Due to the lack of experimental data supporting its role in the catalytic mechanism, the proposed oxyanion hole in cysteine proteases did not benefit from the wide acceptance enjoyed by its serine protease counterpart (Ménard & Storer, 1992). However, the controversy regarding the existence of an operational oxyanion hole in cysteine proteases was resolved when direct experimental evidence for its contribution to catalysis was obtained from site-directed mutagenesis experiments on residue Gln19 of papain (Ménard et al., 1991a). Mutation of Gln19 to alanine and serine leads to 60- and 600-fold decreases in k_{cat}/K_M, respectively, from which the side chain of Gln19 can be estimated to contribute 2.4−3.8 kcal/mol to transition state stabilization. The oxyanion hole therefore seems to be an important part of the catalytic machinery of cysteine proteases.

Additional evidence for the role of the oxyanion hole in the binding of tetrahedral species to the enzyme is found in the X-ray crystallographic structure of a complex between papain and the peptide aldehyde inhibitor leupeptin (Schröder et al., 1993). In the structure of this complex, leupeptin and Cys25 form a hemithioacetal with the oxygen atom sitting within the enzyme's oxyanion hole. Although this observation is supportive of the formation and stabilization of tetrahedral species on the catalytic pathway of cysteine proteases, it is inconsistent with the observation that the mutation of Gln19 to Ala in papain results not in a decrease but in a slight increase in the affinity of the enzyme for aldehyde-based inhibitors (Ménard et al., 1991a). Additional experimentation is necessary to clarify this issue.

Theoretical calculations with trypsin and subtilisin indicate that the nature of the oxyanion hole effect is mostly electrostatic (Warshel & Russell, 1986; Rao et al., 1987; Hwang & Warshel, 1987; Warshel et al., 1989). The oxyanion hole can be viewed as an arrangement of prealigned dipoles that can complement the changes in charge distribution during the enzymatic reaction and gives further support to the idea that electrostatic factors constitute a key aspect of enzyme catalysis (Warshel & Russell, 1984). In this respect, it must be noted that the catalytic center and the oxyanion hole of papain are located at the N-terminal end of an α-helix formed by residues 24−42 and that the Cys25 amide group is actually part of that α-helix. The dipole created by the helix has been proposed to stabilize the ion pair (thiolate−imidazolium) form of the active site residues in papain and also to contribute to the stabilization of the oxyanion in the tetrahedral intermediate (Hol et al., 1978; van Duijnen et al., 1979; Rullmann et al., 1989). Because of the electrostatic nature of the interactions involved in the oxyanion hole, the introduction of charged residues to that region could have a major effect on the catalytic properties of the enzyme.

In previous work with oxyanion hole mutants of papain (Ménard et al., 1991a), Gln19 was replaced by alanine and serine residues to minimize possible unfavorable steric contacts and to avoid introducing new side chains with ionizable groups in the vicinity of the active site. In this study, Gln19 has been replaced by glutamic acid, histidine, and asparagine residues. Glutamic acid is isosteric with glutamine, but possesses a side chain whose charge state is dependent on the pH of the solution. The imidazole side chain of histidine can also be ionized at low pH. With the Gln19Glu, Gln19Asn, and Gln19His mutants, the side chain of residue 19 therefore can be negatively charged, neutral, or positively charged, and this could change the electrostatic environment of the oxyanion hole in a significant fashion. Mutants of subtilisin where the Asn155 residue has been replaced by a histidine or an aspartic acid still display appreciable activity, and it was suggested that the side chain of residue 155 in the Asn155His and Asn155Asp mutants probably moves out into the solvent, therefore minimizing the effect on transition state stability (Wells et al., 1986). The pH dependence of activity for these mutants would provide valuable information, leading to a better understanding of the effect of introducing a charged residue into the oxyanion hole of subtilisin. However, this information can be obtained for papain, as the enzyme is active over a wide range of pH values (pH 3−10), which allows the influence of side chain ionization on activity to be measured in a direct manner with the papain mutants. In this paper, we report the kinetic characterization of the Gln19Glu, Gln19His, and Gln19Asn mutants, as well as the results of molecular modeling experiments aimed at predicting the orientation of the side chains in the mutants. Factors affecting the electrostatic environment of the active site of papain are discussed.

MATERIALS AND METHODS

The substrate CBZ-Phe-Arg-MCA[1] and the irreversible inhibitor E-64 were purchased from IAF Biochem International Inc. (Laval, Québec, Canada). Papain was obtained as the crystallized suspension in sodium acetate from Sigma Chemical Co. and was further purified and activated, and the active site was titrated as described previously (Ménard et al., 1990).

Site-Directed Mutagenesis and Recombinant Protein Expression. All mutants were constructed by site-directed mutagenesis using uracil-containing, single-stranded DNA (Kunkel, 1985) and the following oligonucleotides: GTTAAGAACCACGGCAGCTGT (Gln19His), AGTTAAGAACGAGGGCAGCTGTGG (Gln19Glu), GAACCAAGGCGCTTGTGGTTCTTG (Ser21Ala), and CCAGTTAAGAACAATGGCGCTTGTGGTTCTTG (Gln19Asn/Ser21Ala). Successful mutagenesis with the first two oligonucleotides destroyed a *Sty*I restriction site, whereas the oligo for the Gln19Ser mutation destroyed a *Pvu*II restriction site. Both the *Sty*I and *Pvu*II restriction sites are removed with the oligo for the Gln19Asn/Ser21Ala double mutant. Mutants of papain were expressed either in insect cells (Gln19Glu and Gln19His) infected with recombinant baculoviruses or in *Saccharomyces cerevisiae* (Gln19Asn/Ser21Ala and Ser21Ala). For expression in insect cells, the transfer plasmid IpDC127, containing the papain precursor gene under the control of the polyhedrin promoter, was used (Vernet et al., 1990). Papain precursor mutants were secreted from the insect cells, activated *in vitro*, and then purified (Ménard et al., 1991b).

[1] Abbreviations: CBZ-Phe-Arg-MCA, carbobenzoxy-L-phenylalanyl-L-arginine 4-methylcoumarin-7-amide hydrochloride; E-64, 1-[[(L-*trans*-epoxysuccinyl)-L-leucyl]amino]-4-guanidinobutane; $Glu^{(0)}$ and $Glu^{(-)}$, glutamic acid residue with a side chain in the neutral and ionized states, respectively; $His^{(0)}$ and $His^{(+)}$, histidine residue with a side chain in the neutral and ionized states, respectively; MCA, 7-amino-4-methylcoumarin; oligo(s), oligodeoxynucleotide(s).

Scheme 1

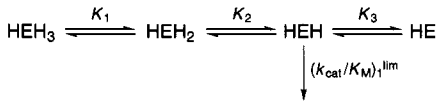

Scheme 2

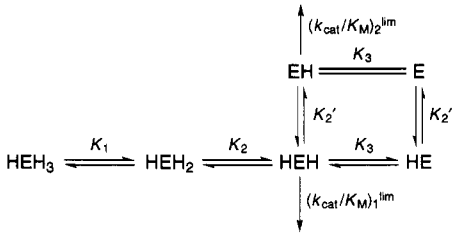

Mutants of the papain precursor gene were also expressed in yeast under the control of the α-factor promoter using plasmid YpDC222 (Vernet et al., 1993). Recovery and purification of the recombinant papain mutants that accumulate in the BJ3501 yeast strain vacuole were performed as described previously (Vernet et al., 1993).

Kinetic Measurements. All kinetic experiments were performed at 25 °C, as previously described, except that 10% CH_3CN was used in the assay mixture. The kinetic parameters k_{cat},[2] K_M, and k_{cat}/K_M, at pH 6.5, were determined by initial rate (v) measurements and linear regression of the data to s/v vs s plots. For pH−activity profiles, the substrate concentration was kept well below K_M, such that k_{cat}/K_M could be obtained simply by dividing the initial rate by the enzyme and substrate concentrations. The pH−activity profile of papain can be described by Scheme 1, where three ionizable groups are considered to modulate the activity (Ménard et al., 1990). It was found that, in addition to wild-type papain, the mutants Gln19His and Gln19Asn also displayed pH dependencies of activity that could be represented by Scheme 1. The kinetic parameters in Scheme 1 have been determined by nonlinear regression of the pH−activity data to eq 1. However, in cases where pK_1 cannot be measured (for example, if $pK_1 \ll pK_2$), the equation used for the nonlinear regression does not contain the term $[H^+]^2/K_1K_2$ in the denominator.

$$k_{cat}/K_M = \frac{(k_{cat}/K_M)_1^{lim}}{\frac{[H^+]^2}{K_1K_2} + \frac{[H^+]}{K_2} + 1 + \frac{K_3}{[H^+]}} \quad (1)$$

For the mutant Gln19Glu, ionization of the Glu side chain has been found to have an influence on the activity of the enzyme. Therefore, the pH−activity profile of the Gln19Glu mutant is best described by Scheme 2, where pK_2' reflects the ionization of Glu19, and two forms of the enzyme (HEH and EH) are active toward the substrate CBZ-Phe-Arg-MCA. The kinetic parameters from the pH−activity profile of Gln19Glu have been obtained by nonlinear regression to eq 2.

$$k_{cat}/K_M = \frac{(k_{cat}/K_M)_1^{lim}}{\frac{[H^+]^2}{K_1K_2} + \frac{[H^+]}{K_2} + \left(1 + \frac{K_3}{[H^+]}\right)\left(1 + \frac{K_2'}{[H^+]}\right)} + \frac{(k_{cat}/K_M)_2^{lim}}{\frac{[H^+]^3}{K_1K_2K_2'} + \frac{[H^+]^2}{K_2K_2'} + \left(1 + \frac{K_3}{[H^+]}\right)\left(1 + \frac{[H^+]}{K_2'}\right)} \quad (2)$$

Computer Modeling. The Systematic Search module of Sybyl 6.0 (Tripos Assoc., Inc.) was used to obtain low-energy conformations of the Gln19 mutant side chains in the active site of a tetrahedral oxyanion intermediate used as a transition state model. This model was built from the crystal structure of a tetrahedral thiohemiacetal complex formed between papain and leupeptin (Schröder et al., 1993). In the model, the hydrogen atom of the hemithioacetal was replaced by the fragment ($NHCH_3$) to represent the leaving group of an amide substrate. In a first step, AMBER partial charges were assigned to the atoms in the model. The active site His159 residue was considered to be in the protonated charge state. Charges for the oxyanion and neighboring atoms were then obtained from a calculation on the small molecule,

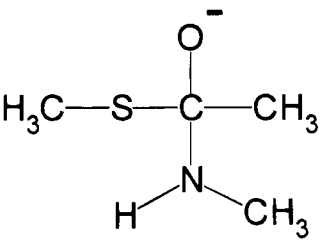

The structure of this molecule was optimized using the MOPAC 6.0 module of Insight (Biosym Tech.), and the electrostatic potential (ESP)-fitted charges were calculated using the Gaussian 92 series of programs (Frisch et al., 1992). The basis set used was 6-31+G*, and the value obtained for the oxygen atom in the oxyanion was −1.005. The ESP-fitted charges were assigned to the appropriate atoms in Cys25 and Arg, followed by the normalization of all charges in Cys25 and Arg using

$$q = q_0 + \Delta q \frac{|q_0|}{\sum |q_0|} \quad (3)$$

where q_0 is the initial charge and Δq is the difference between the target total charge of the two residues and the sum of the q_0 charges.

The transition state model was assumed to have a structure similar to that of the papain−leupeptin complex and the model was energy minimized, allowing movement of the *N*-methyl fragment to position the leaving group. In the minimized structure, the *N*-methyl portion of the molecule is located in the expected S′ subsite of the enzyme. The subsequent conformational searches and energy calculations for the Gln19 mutants were carried out on a region delimited by a sphere of 10 Å around atoms $O_{\delta 1}$ and $N_{\delta 2}$ of the Gln19 side chain in the wild-type enzyme structure. The Gln19 residue was replaced by Asn, Glu, and His (the latter two as their neutral and ionized forms), and the side chain angles χ_1 and χ_2 (Asn, His) and χ_1, χ_2, and χ_3 (Glu) were varied by 1 deg increments. The single point conformational energies

[2] The following conventions are used to describe kinetic data: k_{cat}, K_M, and k_{cat}/K_M represent values of the kinetic parameters determined experimentally; $(k_{cat}/K_M)_1^{lim}$ and $(k_{cat}/K_M)_2^{lim}$ are limiting values of the specificity constant for two different protonic forms of the enzyme, obtained by nonlinear regression of pH − (k_{cat}/K_M) data to a specified equation, while pK_i represents the corresponding experimental pK_a's.

Table 1: Kinetic Parameters for the Hydrolysis of CBZ-Phe-Arg-MCA by Mutant and Wild-Type Papain at pH 6.5

enzyme	k_{cat} (s^{-1})	K_M (mM)	k_{cat}/K_M ($\times 10^3$ M^{-1} s^{-1})	r	f
Gln19Glu	1.58 ± 0.16	0.224 ± 0.023	7.1 ± 1.1		
Gln19His	0.047 ± 0.015	0.032 ± 0.007	1.48 ± 0.28	0.05	0.016
Gln19Asn[a]	1.20 ± 0.10	0.243 ± 0.036	4.93 ± 0.64	0.44	0.013
Gln19Ala[b]	2.4 ± 1.5	0.30 ± 0.10	7.7 ± 2.2	0.53	0.019
Gln19Ser[b]	0.23 ± 0.15	0.27 ± 0.13	0.76 ± 0.24	0.37	0.002
papain	41.6 ± 6.8	0.0892 ± 0.0062	464 ± 44	1	1

[a] This enzyme is a double mutant: Gln19Asn/Ser21Ala. The Ser21Ala mutation was made to avoid introducing a glycosylation site. The single mutation Ser21 to Ala had no effect on activity or the pH profile (data not shown). [b] From Ménard et al. (1991a).

Table 2: Analysis of pH−Activity Profiles for the Hydrolysis of CBZ-Phe-Arg-MCA by Mutant and Wild-Type Papain

enzyme	model[a]	pK_1	pK_2	pK_2'	pK_3	$(k_{cat}/K_M)_1^{lim}$ (M^{-1} s^{-1} × 10^{-3})	$(k_{cat}/K_M)_2^{lim}$ (M^{-1} s^{-1} × 10^{-3})
Gln19Glu	2	3.76 ± 0.27	4.37 ± 0.13	6.02 ± 0.06	8.86 ± 0.17	23.4 ± 3.1	1.87 ± 0.17
Gln19His	1		5.48 ± 0.06		8.09 ± 0.10	1.64 ± 0.31	
Gln19Asn	1	4.03 ± 0.01	4.99 ± 0.04		8.37 ± 0.03	5.15 ± 0.33	
Gln19Ala[b]	1	4.1 ± 0.2	5.02 ± 0.04		8.51 ± 0.05	8.0 ± 2.3	
Gln19Ser[b]	1		5.04 ± 0.03		8.33 ± 0.07	0.80 ± 0.25	
papain	1	3.58 ± 0.29	4.54 ± 0.29		8.45 ± 0.02	482 ± 46	

[a] Minimum model describing the pH−activity profile. The parameters were obtained by nonlinear regression of the data to the corresponding equations, as described in the text. [b] From Ménard et al. (1991a).

were calculated using the Tripos force field with AMBER partial charges. A distance dependent dielectric constant, $\epsilon = r$, was used with a residue-based cutoff distance of 8.0 Å. A number of allowed conformations were found and ranked in order of increasing energy. The lower energy structures were examined to ensure that two conformations of similar energy but widely different side chain orientations were not present.

RESULTS AND DISCUSSION

The kinetic parameters for hydrolysis of the substrate CBZ-Phe-Arg-MCA by the Gln19Glu, Gln19His, and Gln19Asn mutants at pH 6.5 (the optimum pH for wide-type papain) are given in Table 1. It can be seen that the mutations carried out in this work result in 65−315-fold decreases in k_{cat}/K_M, supporting our previous finding that the side chain of Gln19 contributes to transition state stabilization in the oxyanion hole of papain (Ménard et al., 1991a). The results previously obtained for mutants Gln19Ala and Gln19Ser are also reported in Table 1 for comparison. For the five mutants characterized, the decrease in k_{cat}/K_M is mainly due to a decrease in k_{cat}, while K_M is approximately 3-fold higher compared to wild-type papain for all mutants, with the exception of Gln19His, for which K_M decreases 3-fold. Gln19His also displays the lowest k_{cat} value in this collection of enzymes (0.047 s^{-1}, 890-fold lower than the value for the wild type) and has the second lowest k_{cat}/K_M after Gln19Ser, which is the least active mutant.

The pH−activity profile for mutant Gln19Asn can be described by model 1, and the pK_a's of the three groups modulating the activity of the enzyme are reported in Table 2. It can be seen that these pK_a's are, within experimental error, identical to those determined from the Gln19Ala and Gln19Ser pH−activity profiles. For all three mutants, the pH−activity profile is significantly narrower and shifted to a slightly higher pH than that of wild-type papain. For the Ala and Ser mutants, it has been suggested that the narrowing of the profile could be due to the removal of the Gln19−Ser176 interdomain hydrogen bond since a Ser176 to Ala mutation had the same effect (Ménard et al., 1991a). However, molecular modeling experiments with the Gln19Asn mutant suggest that the Asn at position 19 retains the hydrogen bond with the Ser176 side chain (see Figure 1), indicating that this explanation might not be valid. It is most likely that the modification of the pH−activity profile reflects small perturbations in the electrostatic environment of the active site and in the thiolate−imidazolium ion pair stability (Ménard et al., 1991a). An interesting feature of the computer-modeled Gln19Asn mutant is the presence of a hydrogen bond between $N_{\delta 2}$-H of the Asn19 side chain and the carbonyl oxygen of Gly20 (Figure 1). It must be noted that the conformation of the Asn19 side chain displayed in Figure 1 for the tetrahedral intermediate model is almost identical to that obtained by modeling experiments with the free enzyme (data not shown). The existence of the Asn19−Gly20 hydrogen bond in combination with the Asn19−Ser176 interaction orients the side chain upward in the

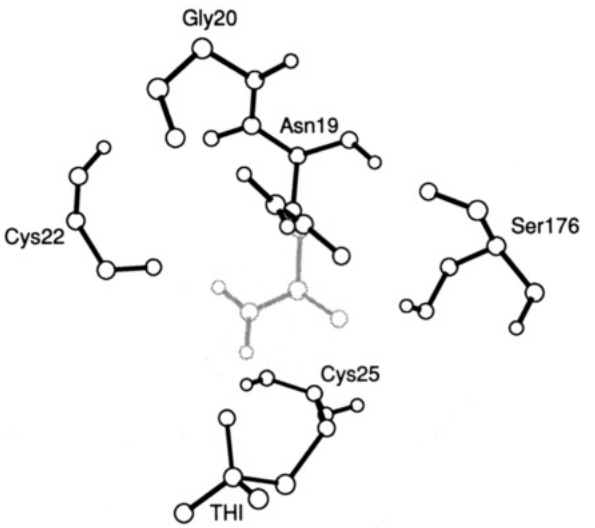

FIGURE 1: Computer modeling prediction of the orientation of the Asn19 side chain in the active site of a tetrahedral oxyanion intermediate used as a transition state model for the mutant Gln19Asn. The Gln19 side chain in wild-type enzyme is represented in light gray. The model was derived using the X-ray crystallographic coordinates from the Brookhaven Protein Data Bank for the structure of a papain−leupeptin complex (Schröder et al., 1993). Details are given in the text.

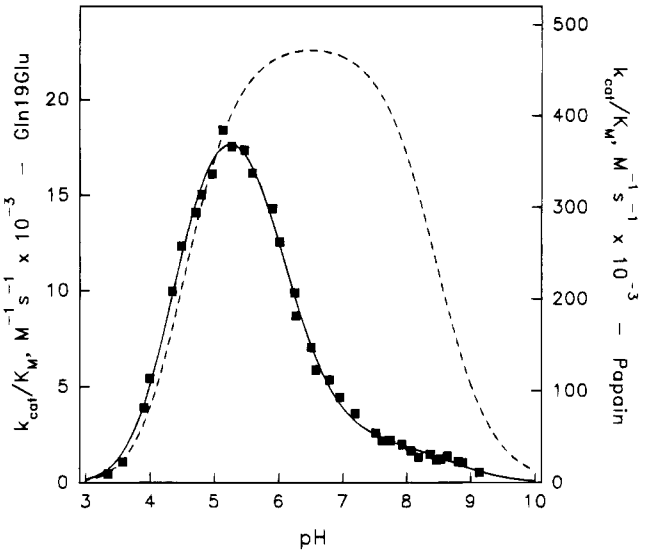

FIGURE 2: pH dependence of k_{cat}/K_M for the Gln19Glu mutant. The solid line represents the best fit to Scheme 2, and the dashed line is the best fit to Scheme 1 for data (not shown) obtained with wild-type papain.

oxyanion hole and creates a larger cavity than if the side chain were pointing down to the active site. The size of this cavity is similar to that formed by the Gln19Ala and Gln19Ser mutants, which could explain the similarity of the pH–activity profiles for these three mutants, as well as the fact that Gln19Asn and Gln19Ala display the same level of activity (i.e., k_{cat}/K_M values of 4.93×10^3 and 7.7×10^3 M^{-1} s^{-1}, respectively). The Gln19Ser mutant, however, has a much lower activity, possibly reflecting differing degrees of solvation for these mutants.

The pH–activity profiles of the Gln19Glu and Gln19His mutants are particularly interesting because the charge state of the side chain introduced at position 19 could change within the pH range where the enzyme is normally active. The pH–activity profile obtained for Gln19Glu is illustrated in Figure 2. The profile is not of the classical bell-shaped form normally observed for papain, but instead can be divided into a region of maximal activity at low pH and a region of lower activity at high pH. This clearly shows that the enzyme possesses at least two protonation states of different but non-negligible activities, as represented by model 2. These two states differ by the ionization of a group that can be accounted for by an additional pK_a in the model (pK_2'). In the Gln19Glu mutant, the additional ionizable group relative to papain is almost certainly the side chain carboxylic acid of Glu19. The pH–activity profile for Gln19Glu has been analyzed according to model 2 by nonlinear regression of the data to eq 2, and the results are given in Table 2. It can be seen that $(k_{cat}/K_M)_1^{lim}$, which reflects the activity of the enzyme when the Glu19 side chain is neutral, is only 20-fold lower than $(k_{cat}/K_M)_1^{lim}$ for wild-type papain. The Gln19Glu mutant with the nonionized Glu19 side chain therefore is the enzyme that displays activity closest to that of the wild-type enzyme. It must also be noted that the pK_a's describing the acid limb of the profile (i.e., pK_1 and pK_2) are, within experimental error, equal to the corresponding pK_a's of the wild-type enzyme.

The characteristics of the Gln19Glu mutant at low pH therefore are somewhat similar to those of wild-type papain, even though the activity is 20-fold lower. As expected, when the Glu19 side chain ionizes, leading to enzyme form EH in Scheme 2, the activity decreases significantly. The observation that the activity of Gln19Glu against CBZ-Phe-Arg-MCA is modulated by ionization of the Glu19 side chain supports the conclusion that the side chain of Gln19 interacts with the substrate in the oxyanion hole of papain. The $(k_{cat}/K_M)_2^{lim}$ for the enzyme with the Glu19 side chain present as a negatively charged glutamate is 1.87×10^3 M^{-1} s^{-1}, a value 260-fold lower than that of wild-type papain. In addition, deprotonation of the active site His159 occurs with a pK_a of 8.86, compared to 8.45 for the wild-type enzyme. At the pH values where His159 deprotonates, Glu19 is present mostly in the negatively charged carboxylate stage, and the shift in pK_2 reflects the electrostatic effect of introducing a negative charge into the environment of His159, as previously observed for other mutants of papain (Ménard et al., 1991b).

The relatively broad pH–activity profile of papain and its near-neutral optimum pH make the determination of the activity of the Gln19Glu mutant in the two ionization states of Glu19 possible and allow quantitative measurement of the effect on activity of introducing a negative charge into the oxyanion hole of papain. By comparing $(k_{cat}/K_M)_1^{lim}$ and $(k_{cat}/K_M)_2^{lim}$, it can be seen that upon going from the neutral Glu19 side chain at low pH to the negatively charged glutamate at higher pH, the activity of the enzyme decreases by only a factor of 12. This result seemed surprising at first, as one might expect that the introduction of a negatively charged group in the vicinity of an oxyanion developing in a tetrahedral transition state would be highly unfavorable and lead to a significant decrease in transition state stability, and therefore to a major loss of activity. However, the Gln19Glu mutant with the Glu19 side chain ionized is relatively active, with a $(k_{cat}/K_M)_2^{lim}$ of 1.87×10^3 M^{-1} s^{-1}. In particular, the Gln19Glu mutant at high pH is still more active than the Gln19Ser enzyme and only 3-fold less active than Gln19Asn. To explain this observation, one must consider the possibility that, upon ionization, the Glu19 side chain does not stay in the vicinity of the oxyanion, but instead moves out of the oxyanion hole and away from the negative charge on the tetrahedral intermediate. To verify that such a movement is possible, molecular modeling experiments were carried out for the two ionization states of Glu19 in the Gln19Glu mutant. For $Gln19Glu^{(0)}$ (the mutant where residue Glu19 is neutral), the predicted orientation of the Glu19 side chain is similar to that of Gln19 in wild-type papain (Figure 3a): the hydrogen bond with Ser176-O_γ is maintained, and the $Glu^{(0)}19$ side chain can act as a hydrogen bond donor to stabilize the oxyanion (2.64 Å between $Glu^{(0)}$-19-$O_{\epsilon 2}$ and the oxyanion). This is in agreement with the previous observation that the Gln19Glu mutant at low pH displays kinetic characteristics very similar to those of wild-type papain. In the lowest energy structure for $Gln19Glu^{(-)}$ (Figure 3b), the negatively charged Glu19 side chain clearly moves away from the oxyanion and forms two hydrogen bonds with neighboring residues (GluH19-$O_{\epsilon 1}$–Ser176-O_γ and GluH19-$O_{\epsilon 1}$–Trp177-$N_{\epsilon 1}$). However, both oxygen atoms in the $Glu^{(-)}19$ side chain are still located relatively close to the oxyanion (approximately 4 Å). Solvation of the ionized Glu19 side chain could also contribute to mask the effect on activity of introducing a negatively charged residue into the oxyanion hole of papain. The importance of solvation of the charged groups has been noted in a recent

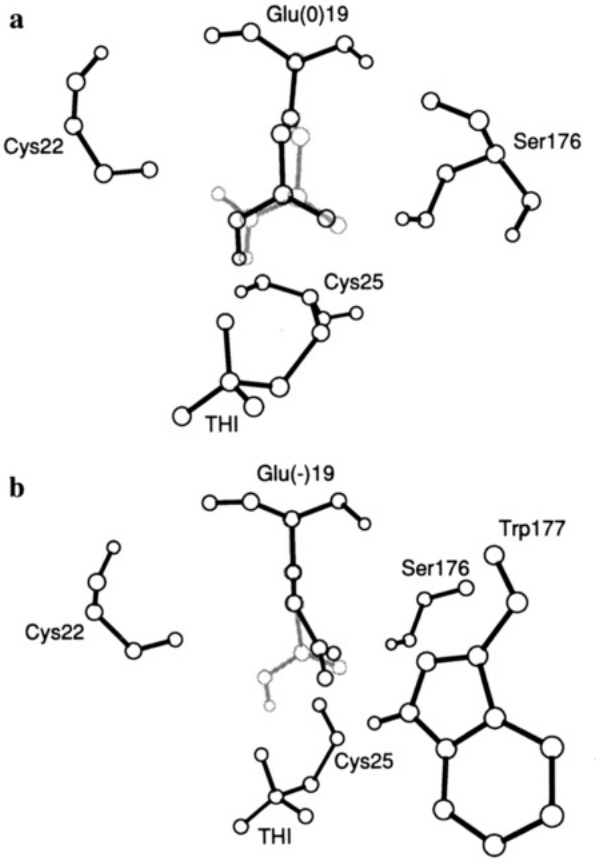

FIGURE 3: Computer modeling prediction of the orientation of the Glu19 side chain in the active site of a tetrahedral oxyanion intermediate used as a transition state model for the mutant Gln19Glu: (a) nonionized $Glu^{(0)}$ side chain (the Gln19 side chain in wild-type enzyme is represented in light gray); (b) ionized $Glu^{(-)}$ side chain (the nonionized $Glu^{(0)}19$ side chain from part a is represented in light gray. Only side chains starting from C_α are shown for Cys25, Ser176, and Trp177 in part b. The model was derived using X-ray crystallographic coordinates from the Brookhaven Protein Data Bank for the structure of a papain−leupeptin complex (Schröder et al., 1993). Details are given in the text.

theoretical study by Dijkman et al. (1991), which indicates that the electrostatic influence of Asp158 determined from calculations performed *in vacuo* is nearly completely screened by the solvent, a finding in agreement with experimental results (Ménard et al., 1991b). Alternatively, the structure of the transition state in papain-catalyzed hydrolysis might be different from that of the papain−leupeptin complex.

As shown in Table 2, the pK_a of the Glu19 side chain in Glu19Glu is relatively high, with $pK_2' = 6.02$. Since it was obtained from the pH dependence of the kinetic parameter k_{cat}/K_M, this pK_a describes the ionization of Glu19 in the free enzyme (Fersht, 1985). The oxyanion hole in papain is located at the N-terminal end of an α-helix constituted by residues 24−42 (Baker & Drenth, 1987). Even though Gln19 is not part of that helix, the amide side chain of Gln19 is located in the vicinity of the α-helix. The dipole resulting from the aligned peptide units of the helix has been proposed to stabilize the active site thiolate−imidazolium ion pair, as well as the tetrahedral intermediate in the catalytic pathway (Hol et al., 1978; van Duijnen et al., 1979; Hol, 1985; Rullmann et al., 1989). Direct involvement of the α-helix dipole in transition state stabilization is difficult to prove experimentally; however, a database has been accumulated on the electrostatic influence of the helix dipole on a charge

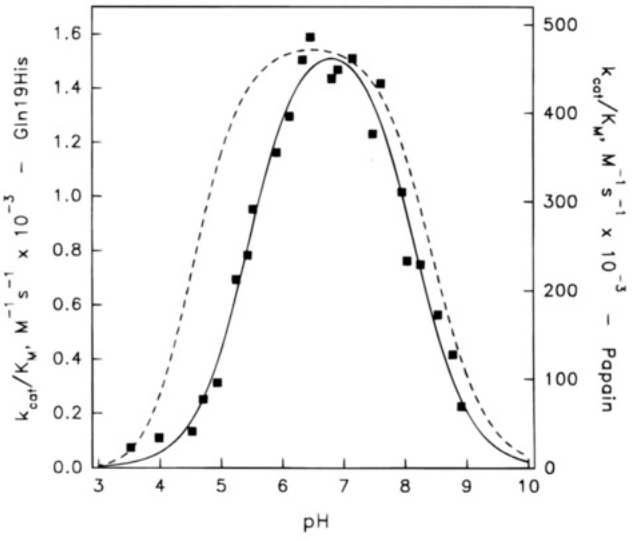

FIGURE 4: pH dependence of k_{cat}/K_M for the Gln19His mutant. The solid line represents the best fit to Scheme 1 without the first ionization step (i.e., only one pK_a in the acid limb), and the dashed line is the best fit to Scheme 1 for data (not shown) obtained with wild-type papain.

near both the C- and N-terminal parts of an α-helix [e.g., Hol (1985)]. In particular, the pK_a of ionizable groups located at the end of an α-helix has been shown to be perturbed compared to normal pK_a's in solution [e.g., Sancho et al. (1992)]. It must be noted, however, that the side chain of Gln19 in wild-type papain is not in the axis of the helix and is also located in the vicinity of the active site thiolate−imidazolium ion pair.

It has been suggested, on the basis of theoretical consideration, that a charged residue close to the N-terminus of an α-helix (i.e., Cys25) can dominate the dipole potential of the helix (Sheridan & Allen, 1980). The pK_a obtained for the Glu19 side chain indicates that the electrostatic potential field in that region of the protein is indeed dominated by the negative charge of the thiolate anion of Cys25 and not by the helix dipole potential, i.e., the electrostatic contribution from the Cys25 thiolate anion is responsible for the high pK_a value of the Glu19 side chain. If only the helix dipole were interacting with Glu19, the pK_a of the side chain would be expected to be lower than normal values, as observed, for example, for aspartic acid residues introduced by site-directed mutagenesis and located at the N-terminal end of α-helices in T4 lysozyme (Nicholson et al., 1988). Alternatively, since the potential resulting from the α-helix dipole falls off rapidly as the distance increases from the terminal dipole (Hol et al., 1978), the present finding could be interpreted to suggest that the side chain of residue 19 in the Gln19Glu-free enzyme moves away from the active site, as it does in the tetrahedral oxyanion model.

The pH−activity profile for the Gln19His mutant is illustrated in Figure 4. The profile can be described by Scheme 1, and contrary to the Gln19Glu mutant, the profile is bell-shaped (within experimental error), with no clear evidence for an additional ionizable group affecting the activity in the range pH 4−9. The pK_a's determined by nonlinear regression are given in Table 2. It can be seen that the values $pK_2 = 5.48$ and $pK_3 = 8.09$ are, respectively, the highest and lowest values determined for these parameters, and the profile therefore is significantly narrower than those of wild-type papain or the other Gln19 mutants.

Assuming that these pK_a's reflect the ionization of the same groups as in wild-type papain (see below), this can be interpreted as an indication that the Gln19 to His mutation has a stronger destabilizing effect on the active site thiolate–imidazolium ion pair, an effect that could also explain, in part, why this enzyme displays a lower activity than the Gln19Ala and Gln19Asn mutants. The width of a pH–activity profile has been used to dissect out the effect of a mutation on ion pair stability and intrinsic activity (Ménard et al., 1991b). The same calculations can be applied in this study for all mutants except Gln19Glu, due to the added complexity of the pH–activity profile introduced by ionization of the Glu19 residue. Table 1 lists the results in terms of the parameters r, which represents the effect of a mutation on the stability of the ion pair, and f, the ratio of intrinsic activity for wild-type to mutant enzymes (Ménard et al., 1991b). The values of f listed in Table 1 indicate that the effect of mutation on intrinsic activity is virtually the same for mutants Gln19His, Gln19Asn, and Gln19Ala. However, ion pair stability is more affected for the Gln19 to His mutation, which results in a lower activity for this mutant relative to Gln19Asn and Gln19Ala. Computer modeling experiments with the mutants Gln19His$^{(0)}$ and Gln19His$^{(+)}$ did not show any favorable interaction being made with the His19 side chain (data not shown). Due to the size of the imidazole ring, the side chain of His19 is more conformationally restrained than that of an asparagine, for example, and steric factors could have an effect on the local protein conformation.

The lack of evidence for an additional ionizable group modulating the activity of the Gln19His enzyme can be explained in a number of ways. The two most obvious possibilities are that ionization of the His19 side chain does not affect enzyme activity or that His19 ionizes with a pK_a outside of the pH range where the enzyme is active. Low pK_a values for histidine residue located at the N-terminal end of an α-helix have been determined for triosephosphate isomerase (Lodi & Knowles, 1993) and barnase (Sancho et al., 1992). Alternatively, if the His19 side chain senses the same environmental effects as the Glu19 side chain in Gln19Glu, then the pK_a of His19 might be higher than 8. Another possibility is that either pK_2 of 5.48 or the pK_3 of 8.09, determined experimentally, corresponds to deprotonation of the His19 side chain. If the latter is the case, the enzyme would be active in only one of the two protonation states of His19. Our results do not allow us to differentiate between these possibilities.

Table 3 lists the change in free energy of transition state stabilization ($\Delta\Delta G^{\ddagger}$) upon mutating residue 19 in papain. The corresponding values obtained for Asn155 mutants of subtilisin are also included for comparison. It can be seen that the oxyanion hole residues, Asn155 (subtilisin) and Gln19 (papain), both play a significant role in the stabilization of the enzyme–substrate transition states formed during catalysis. Although the values for mutants where the Gln amide side chain has been replaced by amino acids with large side chains are less suitable for comparison due to variations in side chain orientation and possible structural modifications, the values of $\Delta\Delta G^{\ddagger}$ for papain given in Table 3 are consistently lower than those for analogous mutations in subtilisin. This suggests that the oxyanion hole in subtilisin might be more important than that in papain. It has been pointed out by Polgar and Asboth (1986) that formation of the oxyanion transition state in cysteine proteases requires only a migration of charge, whereas full charge separation is required for serine proteases and, as a consequence, catalysis by the former relies less heavily on the presence of an oxyanion hole. One notable exception is the mutation to His residue, which leads to a larger decrease in activity for the cysteine protease. This can be attributed to a combination of structural perturbation in papain, as discussed previously, and the possibility of hydrogen bond formation between the His side chain and the oxyanion in subtilisin (Wells et al., 1986).

Table 3: Comparison of the Contribution to Transition State Stabilization of an Oxyanion Hole Residue in Papain and Subtilisin

papain mutant	$\Delta\Delta G^{\ddagger}$ [a] (kcal/mol)	subtilisin mutant[b]	$\Delta\Delta G^{\ddagger}$ (kcal/mol)
Gln19Glu$^{(0)}$	1.8	Asn155His$^{(0)}$ [d]	2.2
Gln19Ala[c]	2.4	Asn155Gln	3.1
Gln19Asn	2.7	Asn155Gly	3.1
Gln19Glu$^{(-)}$	3.3	Asn155Leu	3.4
Gln19His	3.4	Asn155Asp$^{(-)}$ [d]	3.6
Gln19Ser[c]	3.8	Asn155Ala	4.2
		Asn155Ser	4.3
		Asn155Thr	4.8

[a] $\Delta\Delta G^{\ddagger} = -RT \ln[(k_{cat}/K_M)^{lim}_{mutant}/(k_{cat}/K_M)^{lim}_{wild\text{-}type}]$. [b] From Wells et al. (1986), Bryan et al. (1986), Carter and Wells (1990), and Braxton and Wells (1991). [c] From Ménard et al. (1991a). [d] Since the experiment was done at pH 8.6, the His side chain and the Asp side chain are considered to be neutral and negatively charged, respectively.

The results of this study, in addition to providing further support for the contribution of the Gln19 side chain to transition state stabilization in cysteine proteases, demonstrate that ionizable side chains, and in particular a negatively charged glutamate residue, can be accommodated in the oxyanion hole of papain without a drastic reduction in activity. Given that the contribution of the oxyanion hole to transition state stabilization is considered to be mostly electrostatic, these results form a basis, as in the case of serine proteases, for detailed theoretical calculations (Rao et al., 1987; Hwang & Warshel, 1987; Warshel et al., 1989).

ACKNOWLEDGMENT

We thank Drs. Enrico Purisima and Shahul Nilar for their help with molecular modeling.

REFERENCES

Baker, E. N., & Drenth, J. (1987) in *Biological Macromolecules and Assemblies, Volume 3—Active Sites of Enzymes* (Jurnak, F. A., & McPherson, A., Eds.) pp 314–367, John Wiley & Sons, New York.

Braxton, S., & Wells, J. A. (1991) *J. Biol. Chem. 266*, 11797–11800.

Bryan, P., Pantoliano, M. W., Quill, S. G., Hsiao, H.-Y., & Poulos, T. (1986) *Proc. Natl. Acad. Sci. U.S.A. 83*, 3743–3745.

Carter, P., & Wells, J. A. (1990) *Proteins: Struct., Funct., Genet. 7*, 335–342.

Dijkman, J. P., & van Duijnen, P. T. (1991) *Int. J. Quant. Chem.: Quant. Biol. Symp. 18*, 49–59.

Drenth, J., Swen, H. M., Hoogenstraaten, W., & Sluyterman, L. A. Æ. (1975) *Proc. K. Ned. Akad. Wet., Ser. C 78*, 104–110.

Drenth, J., Kalk, K. H., & Swen, H. M. (1976) *Biochemistry 15*, 3731−3738.
Fersht, A. R. (1985) in *Enzyme structure and mechanism*, pp 155−175, W. H. Freeman and Co., New York.
Frisch, M. J., Trucks, G. W., Head-Gordon, M., Gill, P. M. W., Wong, M. W., Foresman, J. B., Johnson, B. G., Schlegel, H. B., Robb, M. A., Replogle, E. S., Gomperts, R., Andres, J. L., Raghavachari, K., Binkley, J. S., Gonzalez, C., Martin, R. L., Fox, D. J., Defrees, D. J., Baker, J., Stewart, J. J. P., & Pople J. A. (1992) *Gaussian 92, Revision E.1*, Gaussian, Inc., Pittsburgh, PA.
Henderson, R. (1970) *J. Mol. Biol. 54*, 341−354.
Hol, W. G. J. (1985) *Prog. Biophys. Mol. Biol. 45*, 149−195.
Hol, W. G. J., van Duijnen, P. T., & Berendsen, H. J. C. (1978) *Nature 273*, 443−446.
Hwang, J.-K., & Warshel, A. (1987) *Biochemistry 26*, 2669−2673.
Kunkel, T. A. (1985) *Proc. Natl. Acad. Sci. U.S.A. 82*, 488−492.
Lodi, P. J., & Knowles, J. R. (1993) *Biochemistry 32*, 4338−4343.
Ménard, R., & Storer, A. C. (1992) *Biol. Chem. Hoppe-Seyler 373*, 393−401.
Ménard, R., Khouri, H. E., Plouffe, C., Dupras, R., Rippoll, D., Vernet, T., Tessier, D. C., Laliberté, F., Thomas, D. Y., & Storer, A. C. (1990) *Biochemistry 29*, 6706−6713.
Ménard, R., Carrière, J., Laflamme, P., Plouffe, C., Khouri, H. E., Vernet, T., Tessier, D. C., Thomas, D. Y., & Storer, A. C. (1991a) *Biochemistry 30*, 8924−8928.
Ménard, R., Khouri, H. E., Plouffe, C., Laflamme, P., Dupras, R., Vernet, T., Tessier, D. C., Thomas, D. Y., & Storer, A. C. (1991b) *Biochemistry 30*, 5531−5538.
Nicholson, H., Becktel, W. J., & Matthews, B. W. (1988) *Nature 336*, 651−656.
Polgar, L., & Asboth, B. (1986) *J. Theor. Biol. 121*, 323−326.
Rao, S. N., Singh, U. C., Bash, P. A., & Kollman, P. A. (1987) *Nature 328*, 551−554.
Robertus, J. D., Kraut, J., Alden, R. A., & Birktoft, J. (1972) *Biochemistry 11*, 4293−4303.
Rullmann, J. A. C., Bellido, M. N., & van Duijnen, P. T. (1989) *J. Mol. Biol. 206*, 101−118.
Sancho, J., Serrano, L., & Fersht, A. R. (1992) *Biochemistry 31*, 2253−2258.
Schröder, E., Phillips, C., Garmen, E., Harlos, K., & Crawford, C. (1993) *FEBS Lett. 315*, 38−42.
Sheridan, R. P., & Allen, L. C. (1980) *Biophys. Chem. 11*, 133−136.
van Duijnen, P. T., Thole, B. T., & Hol, W. G. J. (1979) *Biophys. Chem. 9*, 273−280.
Vernet, T., Tessier, D. C., Richardson, C., Laliberté, F., Khouri, H. E., Bell, A. W., Storer, A. C., & Thomas, D. Y. (1990) *J. Biol. Chem. 265*, 16661−16666.
Vernet, T., Chatellier, J., Tessier, D. C., & Thomas, D. Y. (1993) *Protein Eng. 6*, 213−219.
Warshel, A., & Russell, S. T. (1984) *Q. Rev. Biophys. 17*, 283−422.
Warshel, A., & Russell, S. T. (1986) *J. Am. Chem. Soc. 108*, 6569−6579.
Warshel, A., Naray-Szabo, G., Sussman, F., & Hwang, J.-K. (1989) *Biochemistry 28*, 3629−3637.
Wells, J. A., Cunningham, B. C., Graycar, T. P., & Estell, D. A. (1986) *Philos. Trans. R. Soc. London A317*, 415−423.

BI942211K